Robust integration of direct air capture in power-to-methane systems: techno-economic feasibility study under uncertainty

Diederik Coppitters[a], Alexis Costa[b], Lionel Dubois[c], Diane Thomas[c], Guy De Weireld[b], Francesco Contino[a]

[a] Institute of Mechanics, Materials and Civil Engineering (iMMC), Université catholique de Louvain (UCLouvain), Place du Levant, 2, 1348 Louvain-la-Neuve, diederik.coppitters@uclouvain.be, ***CA***
[b] Thermodynamics and Mathematical Physics Unit, University of Mons (UMONS), Place du parc 20, 7000 Mons, Belgium
[c] Chemical and Biochemical Process Engineering Unit, University of Mons (UMONS), Place du parc 20, 7000 Mons, Belgium

Abstract:
Direct Air Capture (DAC) technologies extract CO_2 directly from the atmosphere and, therefore, compensate for the emissions from sectors that are difficult to decarbonize, e.g. aviation and heavy-duty mobility. However, due to the diluted CO_2 in the atmosphere, DAC suffers from high costs and a significant energy footprint. When integrating DAC in power-to-gas systems, several underexplored synergies unfold that reduce the energy and water demand of the system, such as waste heat recycling from methanation and water recovery in the DAC unit. Interconnecting these energy and water streams results in a highly integrated system that is fragile towards changes in ambient and operating conditions. We developed a power-to-gas system with solid sorbent direct air capture and evaluated the energy efficiency and water self-sufficiency ratio under uncertain ambient and operating conditions. The results illustrate that operating at a desorption temperature of 61°C, instead of 100°C, results in a water self-sufficient system under average ambient conditions for Belgium, at the expense of a reduction in the energy efficiency of 4% absolute (from 59% to 55%). Considering ambient and operating uncertainties results in a limited uncertainty on the energy efficiency (mean = 59.4%, standard deviation = 0.61%), but a significant uncertainty on the water self-sufficiency ratio (mean = 49.6%, standard deviation = 6.18%). Adopting time series for the ambient conditions is the main action to reduce uncertainty on the quantities of interest. Future work will focus on the dynamic operation of the system, including energy storage and renewable energy technologies.

Keywords:
Direct air capture, methanation, uncertainty quantification, water co-adsorption.

1. Introduction

Energy storage in the form of electrofuels reaches high energy densities when compared to battery storage, which provides significant advantages in weight and volume during seasonal energy storage and long-distance energy transport [1]. Moreover, electrofuels can be used in sectors that are difficult to electrify, e.g., heavy-duty mobility and non-energy demand. Among all electrofuels, Power-to-Gas (PtG) promises a high efficiency (53% to produce and transport methane from renewable electricity [2]), and a methane gas transport grid is already in place. A PtG system mainly consists of a CO_2 source, an electrolyzer and a methanation component. In the methanation component, hydrogen and CO_2 are combined to produce methane [3]. Among the methanation technologies, catalytic methanation in a fixed bed reactor with a Ni-based catalyst is well-established in steady-state operation [1]. Hydrogen is recovered from the electrochemical splitting of water during electrolysis. When the electricity source for electrolysis is intermittent, Proton Exchange Membrane electrolyzers offer significant advantages in terms of flexibility (i.e., full load range) and compactness (i.e., high current densities up to $2\,A/cm^2$) [4]. The CO_2 feedstock generally originates from fossil point sources (e.g., coal-fired power plants or cement production units), renewable point sources (e.g., anaerobic digestion) or the atmosphere, i.e., Direct Air Capture (DAC) [5]. DAC extracts CO_2 from ambient air and can, therefore, be used to offset CO_2 emissions from distributed sources, such as aviation. Roughly, DAC is performed by three technologies: high-temperature (900 °C) liquid scrubbing with an alkaline solution, low-temperature (100 °C) liquid scrubbing with a monoethanolamine solution and low-temperature (100 °C) adsorption and desorption with a solid sorbent. The productivity of the liquid solvent processes is low (below $1\,kg_{CO_2}/(m^3/h)_{air}$) when compared to the solid sorbent process ($3.8\,kg_{CO_2}/(m^3/h)_{air}$ - $10.6\,kg_{CO_2}/(m^3/h)_{air}$) [6].

Solid sorbent DAC systems are mainly studied in isolation, where the aim is to minimize the co-adsorption of water and its corresponding energy penalty [7]. However, integrating DAC in PtG (DAC-PtG) unfolds several underexplored synergies. These synergies include, among others, water recovery in solid sorbent DAC to comply with the water demand of hydrogen electrolysis and recycling waste heat from methanation and electrolysis for DAC. Following these synergies, the energy and water demand of the DAC-PtG process can be reduced substantially [8]. Interconnecting energy and water streams between the DAC-PtG system components results in a highly integrated system that is fragile towards uncertainties in the working environment, i.e., a small change in operating parameters could lead to dramatic decrease in efficiency. Typically, defining these operating parameters in high-fidelity PtG models is based on the expertise of the authors [9], and the ambient conditions are generally fixed based on average conditions over a certain period [10].

To understand the importance of uncertain input parameters on the performance of the system, Uncertainty Quantification (UQ) is typically adopted. The state-of-the-art method that propagates parameter uncertainties through a system model and quantifies the statistical moments of the model output is crude Monte Carlo Simulation (MCS). Despite always-converging and easy to implement, Monte Carlo Simulation converges slowly, i.e., $10^3 - 10^4$ training samples are typically required [11]. Alternatively, surrogate-assisted UQ is gaining interest [12, 13]. In this approach, a surrogate model is constructed for the input-output relation of the system model, based on a set of training samples. Typical surrogate models include Kriging [14] and Polynomial Chaos Expansion (PCE) [15]. Once the surrogate model is constructed, PCE enables to analytically quantify the statistical moments (i.e., mean and standard deviation) and the sensitivity indices (i.e., Sobol' indices) [16]. Coppitters et al. [17] used PCE to quantify the statistical moments on the levelized cost of hydrogen for a directly-coupled photovoltaic-electrolyzer system.

In an isolated evaluation of solid sorbent DAC, the co-adsorption of water is often minimized, to reduce the energy penalty related to the desorption of water. However, when integrated into a PtG system, the co-adsorbed water can cover the water demand during water electrolysis. Moreover, the energy penalty can be compensated by recovering waste heat from the methanation reactor. Despite these strong synergies between the components, such an integrated system is fragile towards uncertainties during system operation. Therefore, we quantified the effect of uncertain ambient and operating conditions on the performance of the PtG system. In Section 2., the PtG system modelling is introduced, followed by an explanation on the characterization of the uncertainties and the UQ method. In Section 3., the performance of the system in steady-state conditions and the effect of uncertainties on that performance is presented. The conclusion in Section 4. closes this article.

2. Methods

The methodology section introduces the modelling of each component in the system, followed by the definition of the quantities of interest. After that, the characterization of the parametric uncertainties is elaborated. The discussion on the PCE method, used to perform UQ on the PtG system, closes this section.

2.1. System model

The PtG system with solid sorbent DAC (DAC-PtG) consists of a methanation unit, electrolyzer and DAC unit (Figure 1). The DAC unit adsorbs CO_2 and water from the ambient air. The co-adsorbed water is used to comply with the water demand of the electrolyzer, which converts water into hydrogen and oxygen. The CO_2 and hydrogen react in a methanation unit and form raw Synthetic Natural Gas (SNG). The waste heat released by this exothermic reaction is recovered as steam to comply with the heat demand of the DAC unit. In this study, an SNG upgrading unit for grid injection is not included.

The model is developed in Python. A validated model is adopted from the literature for each component in the system. These models are integrated into a Python script that initiates the power management strategy and quantifies the quantities of interest.

This modelling is performed using thermodynamic properties adopted from the Python- package CoolProp [18].

2.1.1. Electrolyzer

We adopted the PEM electrolyser technology to convert water into hydrogen by using electricity. A PEM electrolyzer promises a fast response time ($<$1 s) and full operational flexibility, which are significant benefits when coupled to an intermittent energy supply [4]. To model the electrolyzer hydrogen production and corresponding energy consumption, we adopted the model from Abdin et al. [19]. The model quantifies the voltage-current relation as follows:

$$U_{\text{PEM}} = U_{\text{oc}} - U_{\text{act}} - U_{\text{ohm}} - U_{\text{con}}, \tag{1}$$

where the open-circuit voltage U_{oc}, activation overpotential U_{act}, ohmic overpotential U_{ohm} and concentration overpotential U_{con} depend, among others, on the operating temperature, pressure and current. Following this voltage-current relation, the operating current of the electrolyzer can be defined, based on the applied power.

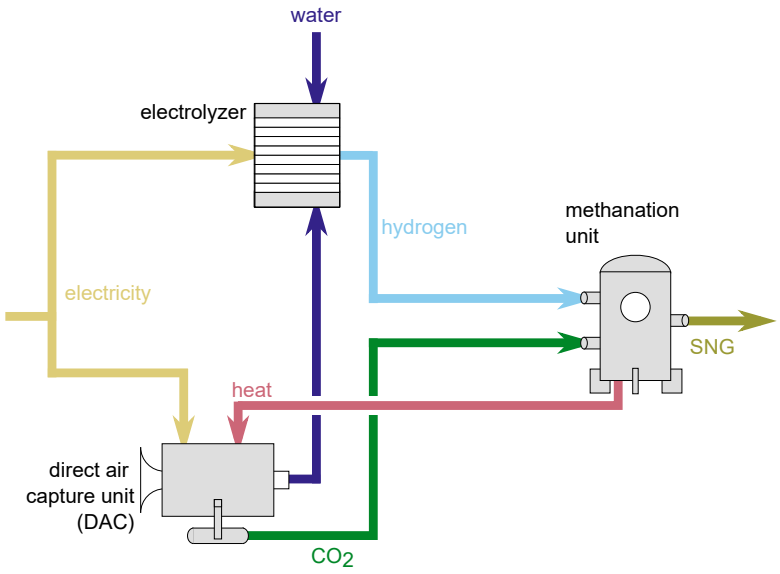

Figure 1: The simplified schematic of the power-to-gas system illustrates that the hydrogen and CO_2 are generated in an electrolyzer and direct air capture unit, respectively. The hydrogen and CO_2 result into Synthetic Natural Gas in the methanation unit.

From this operating current I, the hydrogen molar flow rate $\dot{n}_{H_2}$ can be quantified:

$$\dot{n}_{H_2} = \frac{I}{2F}, \tag{2}$$

where F corresponds to the Faraday constant (96 485 C/mol).

2.1.2. Direct air capture unit

We adopted a low-temperature solid sorbent technology to perform CO_2 capture from the air. The adsorption is performed on a commercially available amine-based sorbent Lewatit VP OC 1065, followed by a desorption step at 100 °C. Compared to high-temperature aqueous solution technologies, the solid sorbent approach requires low-grade heat and does not need a water supply. This technology co-adsorbs water from the air and provides water as an additional product in the output stream. However, the co-adsorption of water is generally minimized, as the heat of desorption of water ($\Delta H_{des,H_2O} \approx 41$ kJ/mol) needs to be complied with as well. The relation between the working capacities of CO_2 and H_2O is quantified based on the respective adsorption isotherms, adopted from Drechsler et al. [20] (Figure 2). The isotherms illustrate that at a desorption temperature of 100 °C, a molar ratio H_2O:CO_2 of 4:1 is expected.

2.1.3. Methanation unit

The methanation unit consists of four series-connected adiabatic fixed-bed reactors. At each reactor, the gas inlet stream temperature is maintained at 350 °C, by cooling down the outlet gas stream from the previous reactor in the series. To reduce the outlet temperature from the first reactor and preheat the incoming H_2 and CO_2 streams, 70 % of the gas at the outlet of the first reactor is recycled. The Gas Hourly Space Velocity (GHSV) is maintained close to 4000 h^{-1}. Finally, the outlet gas stream is cooled down after the fourth reactor, and the remaining water is extracted. Below 600 °C, only the species involved in the Sabatier reaction are present in the outlet stream [9]:

$$CO_2 + 4H_2 \rightleftharpoons CH_4 + 2H_2O \qquad \Delta H_{298} = -165 \text{ kJ/mol}. \tag{3}$$

Therefore, only the Sabatier reaction is considered during methanation. The corresponding reaction rate of CH_4 is obtained by a Langmuir–Hinshelwood–Hougen–Watson approach [9]:

$$r_{CH_4} = -\frac{k}{p_{H_2}^{3.5}} \frac{p_{CH_4}\, p_{H_2O}^2 - \dfrac{p_{H_2}^4\, p_{CO_2}}{K}}{\left(1 + K_{CO} p_{CO} + K_{H_2} p_{H_2} + K_{CH_4} p_{CH_4} + \dfrac{K_{H_2O} p_{H_2O}}{p_{H_2}}\right)^2}, \tag{4}$$

where p corresponds to the partial pressures of the components, k is the rate coefficient depending on the reaction temperature and K_i are the adsorption constants of reaction for the reaction components. We refer to Chauvy et al. [21] for additional details on the design of the methanation unit and the quantification of the parameters in the reaction rate equation.

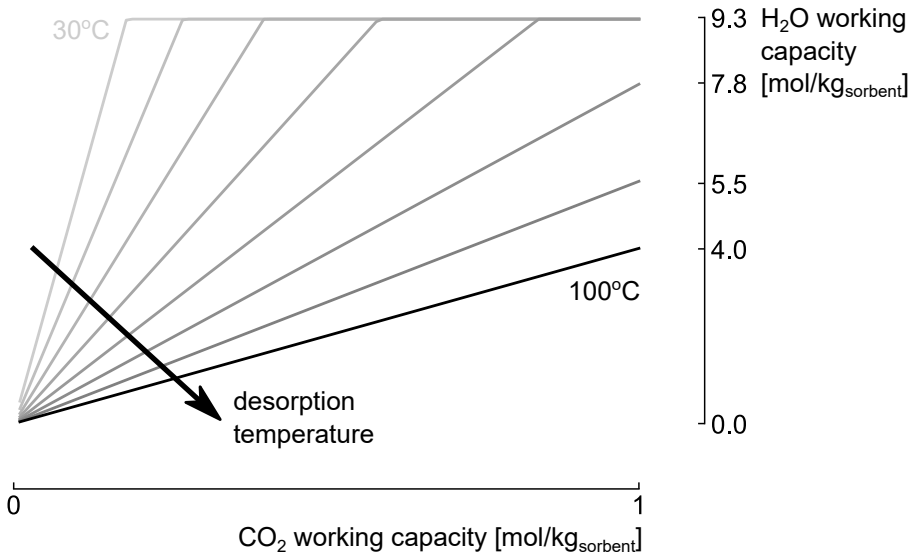

Figure 2: The working capacity of H_2O with respect to the working capacity of CO_2 for different desorption temperatures illustrates that the co-adsorption of H_2O reduces with the increase of desorption temperature. The isotherms are presented at ambient air temperature of 25 °C and 80% relative humidity, at desorption temperature from 30 °C to 100 °C, in steps of 10 °C.

2.1.4. Other components

The PtG system is equipped with compressors, condensers and heat exchangers. These models are adopted from Drechsler et al. [8]. The hydrogen compressor and vapour compressor (i.e., the H_2O and CO_2 mixture leaving the DAC unit) are modelled assuming an ideal gas mixture and an isentropic efficiency of 75 %. After the vapor compressor, the gas is sent to a condenser, which operates at a temperature difference of 10 °C with the desorption process, to ensure a minimal heat transfer driving force (i.e., $T_{\text{cond}} = T_{\text{des}} + 10\,^{\circ}\text{C}$). We assume a phase equilibrium at the condenser outlet (i.e., $p_{H_2O} = p_{H_2O,\text{sat}}(T_{\text{cond}})$), no pressure losses and no heat losses. Finally, for the heat exchangers, heaters and coolers, ideal behaviour is considered: No pressure losses and no heat losses to the environment in the heat exchangers.

2.2. Quantities of interest

The energy efficiency and water self-sufficiency ratio are selected as quantities of interest to illustrate the performance of the DAC-PtG system. The energy efficiency is defined by the electric power consumed by the system, divided by the energy content of the SNG and the remaining heat available in the excess steam:

$$\eta = \frac{E_{\text{in}}}{\text{LHV}_{\text{SNG}} m_{\text{SNG}} + E_{\text{excess heat}}}. \tag{5}$$

The water self-sufficiency ratio indicates the level of self-sufficiency in terms of water supply. In other words, the quantity indicates the amount of water recycled within the DAC-PtG system. While the system requires water for electrolysis and methanation unit cooling purposes, water can be recovered from the DAC ($m_{H_2O,\text{DAC}}$) and methanation unit product stream ($m_{H_2O,\text{demand}}$):

$$\text{SSR}_{H_2O} = \frac{m_{H_2O,\text{DAC}} + m_{H_2O,\text{meth}}}{m_{H_2O,\text{demand}}}. \tag{6}$$

As the water used for cooling purposes in the methanation unit can be supplied to the PEM electrolyzer, $m_{H_2O,\text{demand}}$ corresponds to the water used in the methanation unit, if this quantity is equal or more significant than the amount of water consumed in the PEM electrolyzer. In case the PEM electrolysis consumes more water than the methanation unit cooling, $m_{H_2O,\text{demand}}$ corresponds to the methanation unit cooling water and the difference between the water used for PEM electrolysis and the water used for cooling the methanation unit.

The Levelized Cost Of Energy (LCOE) indicates the system cost per unit of energy in the raw SNG:

$$\text{LCOE} = \frac{\text{CAPEX}_{\text{a}} + \text{OPEX}_{\text{a}} + C_{\text{elec,a}}}{E_{\text{raw-SNG}}}, \tag{7}$$

where $E_{\text{raw-SNG}}$ corresponds to the energy content of the SNG on a LHV-basis, considering both methane and hydrogen contributing to the SNG. We refer to Coppitters et al. [22] for the quantification of the parameters. The assumptions on the economic parameters are listed in Table 1.

Table 1: The cost parameters used in the quantification of the Levelized Cost Of Energy.

parameter	value	unit	Ref.
electricity price	40	€/MWh	[21]
$CAPEX_{PEM}$	1750	€/kW	[4]
$OPEX_{PEM}$	4	% of CAPEX	[4]
$CAPEX_{DAC}$	730	€/t_{CO_2}/year	[23]
$OPEX_{DAC}$	4	% of CAPEX	[23]
$CAPEX_{methanation}$	735	€/kW_{SNG}	[24]
$OPEX_{methanation}$	29	€/kW_{SNG}/year	[24]
interest rate	6	%	[21]

2.3. Uncertainty characterization

To quantify the performance of the DAC-PtG system, several parameters need to be defined, which are intrinsically subject to uncertainty. In this work, seven independent parametric uncertainties are assumed (Table 2). To represent the operation fragility in the different components, the operating temperature of the desorption in the DAC unit, the methanation reaction temperature and the PEM electrolysis operating temperature are defined with a Uniform distribution, due to the lack of specific knowledge on the distribution. The distributions are defined $\pm 5\,^{\circ}$C from the nominal value. In addition, a Uniform distribution is considered on the heat of desorption (ΔH_{des}) of CO_2 and H_2O. Finally, the uncertainty on the relative humidity and ambient temperature represents the uncertainty in the weather conditions, based on a data series of a Typical Meteorological Year in Belgium [25].

Table 2: Uniform uncertainties

Name	parameter 1	parameter 2	unit
Uniform	min	max	unit
relative humidity	60	100	%
desorption temperature	100	110	°C
reaction temperature	345	355	°C
electrolysis temperature	75	85	°C
compressor efficiency	70	80	%
$\Delta H_{des,CO_2}$	70	80	kJ/mol
$\Delta H_{des,H_2O}$	40	42	kJ/mol
Gaussian	mean	std. dev.	unit
ambient temperature	12	3	°C

2.4. Uncertainty quantification

To perform UQ in a computationally-efficient manner, Polynomial Chaos Expansion is adopted to propagate the parametric uncertainties through the system model, quantify the statistical moments on the quantities of interest, and determine the Sobol' indices [26]. PCE represents the input-output relation of the system model in the stochastic space. This representation consists of a truncated series of orthonormal polynomials Ψ_i, scaled by coefficients u_i:

$$\hat{M}(\xi) = \sum_{i=0}^{P} u_i \Psi_i(\xi) \approx M(\xi), \tag{8}$$

where $\xi = \{\xi_1, \ldots, \xi_d\}$ represents the vector of d independent uncertain parameters. The number of terms in the truncated PCE ($P+1$) depends on the maximum total degree p of the multivariate polynomials in the series, and the number of parametric uncertainties considered ($d = 7$):

$$P + 1 = \frac{(p+d)!}{p!d!}. \tag{9}$$

The regression method is adopted to quantify the coefficients for the $P+1$ orthonormal polynomials. To acquire a well-posed least-square minimization, the empirical rule of thumb is to have a number of random samples equal to at least two times the number of coefficients. Hence, $2\,(P+1)$ samples are evaluated in the system

model, and the model response for each quantity of interest is stored. To illustrate, for a total degree $p = 2$ and seven uncertain parameters ($d = 7$), 72 samples are constructed and evaluated in the system model. These training samples are generated using quasi-random Sobol sampling. Once the PCE is built, the statistical moments can be derived from the coefficients analytically, i.e., no more model evaluations are required. To illustrate, the mean μ^{PCE} and standard deviation σ^{PCE} are derived as follows:

$$\mu^{\text{PCE}} = u_0, \tag{10}$$

$$\sigma^{2,\,\text{PCE}} = \sum_{i \neq 0} u_i^2. \tag{11}$$

In addition, the Sobol' indices can be quantified analytically as well. These indices correspond to the sensitivity indices retrieved from a global sensitivity analysis, considering the distributions of the uncertain parameters as inputs for the analysis. The total-order Sobol' indices ($S_i^{T,\text{PCE}}$) quantify the total impact of a stochastic input parameter on the performance indicator, including all interactions:

$$S_i^{T,\text{PCE}} = \sum_{\alpha \in A_i^T} u_\alpha^2 / \sum_{i=1}^{P} u_i^2 \qquad A_i^T = \{\alpha \in A | \alpha_i > 0\}, \tag{12}$$

where A is the set of all the PCE coefficients and α_i represents the coefficient related to uncertain parameter i. Thus, for a total-order Sobol' index related to parameter i, all coefficients are captured for which the value on the position in multi-index α is higher than zero.

3. Results and discussion

First, the flow sheet of the DAC-PtG is presented for fixed ambient and operational conditions, followed by an illustration of the effect of the desorption temperature on the efficiency and water self-sufficiency ratio. After that, the ambient and operating conditions are considered uncertain and propagated through the system model. The effect of the uncertain parameters on both quantities of interest is quantified, and the Sobol' indices are derived.

3.1. System evaluation

To illustrate the operating conditions of the proposed DAC-PtG system, a flow sheet is presented in Figure 3, containing the mass and energy streams between the different components in the PtG system. Air enters the DAC unit at 10 °C and 80 % RH. The DAC unit operates at a desorption temperature of 100 °C, which results in a gas outlet stream containing 968 kg_{CO_2}/h and 406 $\text{kg}_{\text{H}_2\text{O}}$/h. This corresponds to a H_2O:CO_2 molar adsorption ratio of approximately 1:1. The DAC unit requires 0.24 MW_e to cover the power required by the fans, and 0.71 MW_th for the sorbent regeneration. After the DAC unit, a mechanical vapour recompression unit is installed. In this unit, first, the gas is compressed up to 10 bar at an isentropic efficiency of 75 %, requiring 0.43 MW_e. Thereafter, the compressed stream is cooled down to 110 °C, which results in 340 $\text{kg}_{\text{H}_2\text{O}}$ of condensed water (84 % of the inlet water vapour). This process releases 0.31 MW_th of heat, which is supplied to the DAC. Thus, by recovering the water vapour from the DAC product gas, 44 % of the DAC heat demand is complied with. Note that the condensation occurs at 110 °C, to achieve a heat driving force of 10 °C between the heat source and the desorption temperature in the DAC unit. As not all the water is recovered from the DAC unit, the CO_2 stream enters the methanation unit containing water vapour, i.e., 968 kg_{CO_2}/h and 66 $\text{kg}_{\text{H}_2\text{O}}$/h.

Hydrogen is produced in a pressurized PEM electrolyser unit. To produce 180 kg_{H_2}/h, the electrolyzer consumes 10 MW_e and 1620 $\text{kg}_{\text{H}_2\text{O}}$/h. Hence, the PEM electrolyser unit is the main power consuming unit in the DAC-PtG system (93%). The hydrogen is considered pure and enters the methanation unit at 80 °C and 10 bar.

The methanation unit is cooled by evaporating and superheating pressurized water (10 bar, 110 °C) up to 200 °C. In total, 2324 $\text{kg}_{\text{H}_2\text{O}}$/h of coolant is required. The cooling water is divided over five heat exchangers in the methanation unit: one in front of each reactor to cool down the reactor inlet stream to 350 °C, and one to cool down the product stream after the fourth reactor (Figure 4). After the first reactor, 70% of the product stream is recycled (2820 kg/h) to preheat the inlet stream for the first reactor. A compressor is installed to overcome the pressure losses (1 bar) in the recycled stream. The four reactors subsequently increase the content of CH_4 and H_2O in the product stream. However, the increase in mass fraction of these components is reduced in each subsequent reactor, as the equilibrium state is reached. Therefore, the temperature of the product stream after each reactor subsequently reduces: 606 °C after the first reactor, 507 °C after the second reactor, 436 °C after the third reactor and 374 °C after the fourth reactor. Consequently, the amount of coolant water after each reactor is reduced proportionally.

The produced steam can be recycled in the system to comply with the heat demands in the different components: 99 $\text{kg}_{\text{H}_2\text{O}}$/h is condensed to preheat the water recovered from the methanation unit, 200 $\text{kg}_{\text{H}_2\text{O}}$/h is

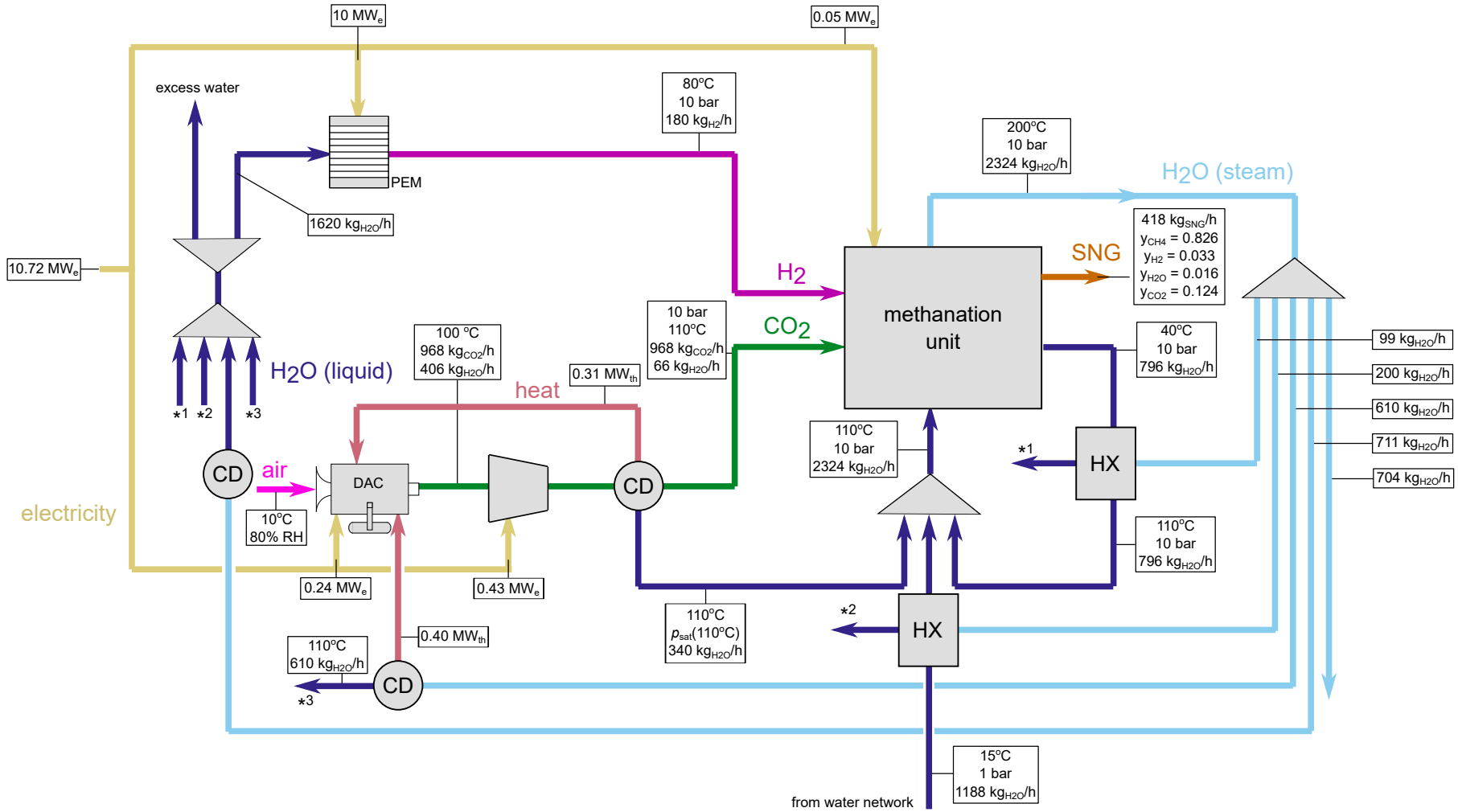

Figure 3: The flowsheet of the power-to-gas system in steady-state operation illustrates that 10.72 MW_e of electric power is consumed, of which the Proton Exchange Membrane (PEM) electrolyzer consumes 10 MW to produce 180 kg_{H_2}/h. With ambient air at 10 °C and 80 % relative humidity, the Direct Air Capture (DAC) unit consumes 0.24 MW_e of power for the fans and 0.71 MW_{th} of thermal energy, to produce 968 kg_{CO_2}/h, accompanied by 406 kg_{H_2O}/h. In the mechanical vapour recompression unit, i.e., the compressor and condenser (CD), 340 kg_{H_2O}/h (84%) is condensed, corresponding to a heat recovery of 0.31 MW_{th}. The liquid water is mixed with liquid water recuperated from the methanation unit and as a coolant in the methanation unit. In the methanation unit, the 2324 kg_{H_2O}/h of coolant is converted into steam and sent to heat exchangers (HX) to preheat the water coolant, and to a CD to recuperate the heat for the DAC system. Thereafter, the water is fed to the PEM electrolyzer unit, and the remaining mass is stored in the water storage tank. Note that the pumps to increase the liquid water pressure are not provided in the schematic.

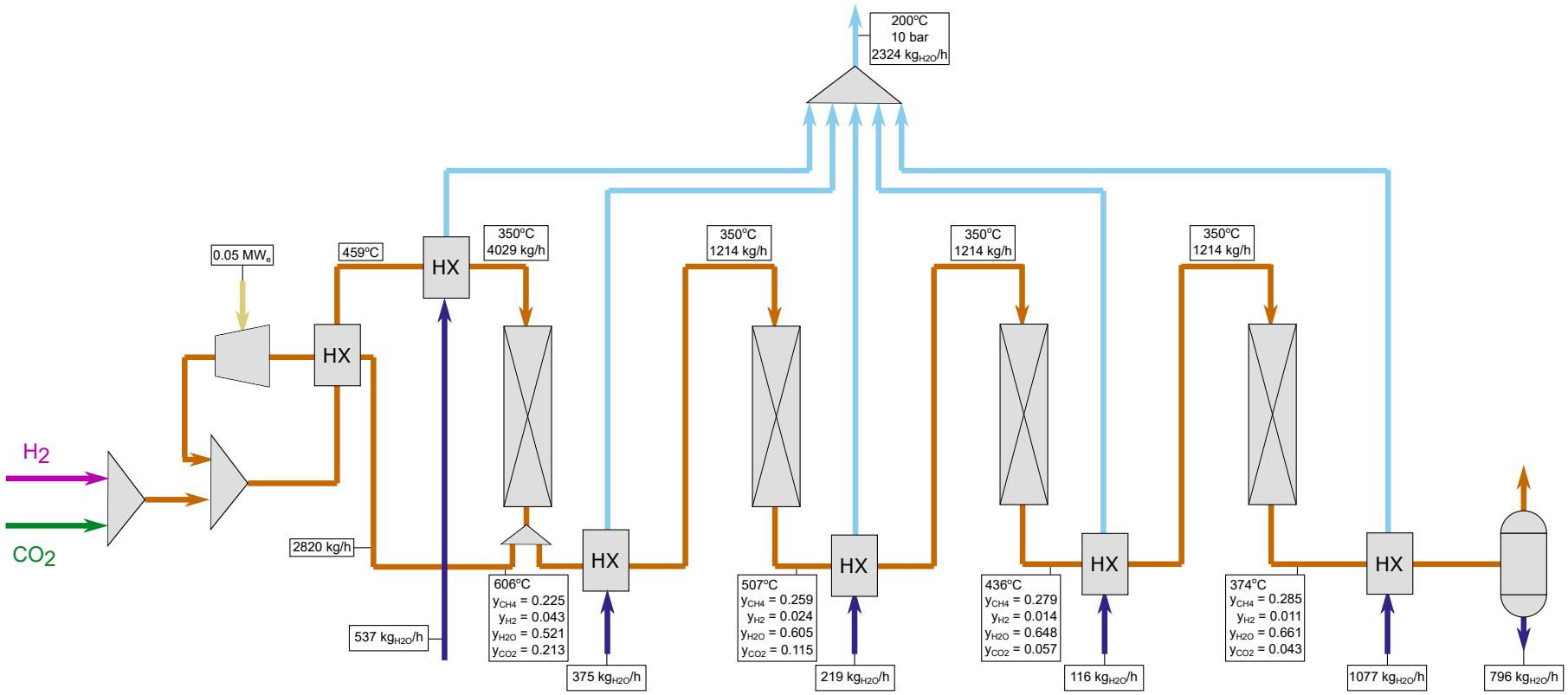

Figure 4: The methanation unit consists of four reactors. In each reactor, the gas mixture enters at 350 °C. After the first reactor, 70% of the gas mixture is recycled. The remaining flow is cooled down in a heat exchanger, where water is evaporated and heated up to 200 °C. After the fourth reactor, the remaining water in the gas mixture is removed through condensation.

condensed to preheat the water from the water network, and 610 kg_{H_2O}/h is condensed to provide the remaining heat for the DAC unit. The remaining available steam (1415 kg_{H_2O}/h) can be used for other purposes outside the DAC-PtG system. Note that 711 kg_{H_2O}/h is condensed to reach the required amount of water for electrolysis, but the released heat during this condensation is not used. Finally, the methanation unit produces 418 kg_{SNG}/h, containing 82.6 $\%_{mass}$ CH_4 and 3.3 $\%_{mass}$ H_2. Considering the SNG energy content and the available excess heat, the system reaches an energy efficiency of 59.5 %. As 1188 kg_{H_2O}/h is extracted from the water network, the water self-sufficiency ratio corresponds to 48.8 %. The LCOE for raw SNG corresponds to 180 €/MWh. This value situates near existing values present in literature: Chauvy et al. [21] performed a techno-economic study on a renewable methanation plant, considering CO_2 capture from a cement plant, and presented a value of 170 €/MWh for raw SNG with similar quality.

The co-adsorption of water mainly determines the water self-sufficiency ratio in the DAC unit. This water co-adsorption depends on the ambient conditions, i.e., ambient temperature and humidity, and the desorption temperature. Generally, the desorption temperature is maximized, to minimize the energy penalty related to the co-adsorption of water. However, reducing the desorption temperature increases the co-adsorption of water and, thus, the water self-sufficiency ratio of the system (Figure 5). Reducing the desorption temperature to 61 °C results in a self-sufficient water system. When compared to a desorption temperature of 100 °C, the energy efficiency is reduced by 4 $\%_{abs}$, i.e., from 59 % to 55 %. Due to the condensation of (a major part of) the water vapour in the DAC product stream, a large part of the heat of evaporation can be recovered, which limits the reduction in energy efficiency when reducing the desorption temperature, and thus, increasing the water co-adsorption- in the DAC unit.

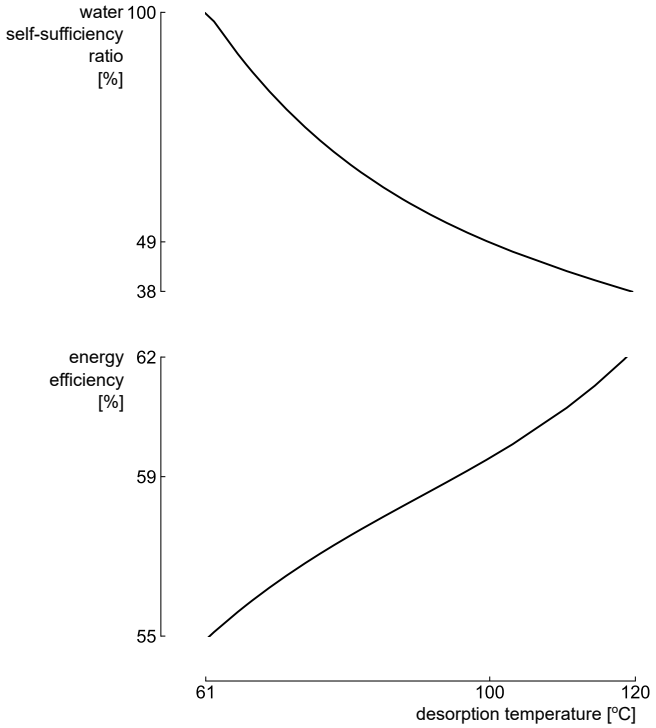

Figure 5: Increasing the desorption temperature slightly improves the energy efficiency, but significantly reduces the water self-sufficiency ratio.

3.2. Uncertainty quantification

The distribution on the energy efficiency (mean = 59.4%, standard deviation = 0.61%) illustrates that the effect of the parametric uncertainties on the energy efficiency is small (Figure 6). The Sobol' indices indicate that the uncertainty on the energy efficiency is mainly driven by the uncertainty on the ambient temperature (0.47), desorption temperature (0.27) and the heat of desorption of CO_2 (0.14). Therefore, to reduce the uncertainty on the efficiency, a time series on the ambient temperature, accurate characterization of the heat of desorption of CO_2 and measures to stabilize the desorption temperature are considered as the main actions.

The water self-sufficiency ratio (mean = 49.6%, standard deviation = 6.18%) is significantly affected by the parametric uncertainties (Figure 7). In this case, the uncertainty on the ambient conditions, i.e., ambient temperature (0.70) and relative humidity (0.21), dominantly drives the uncertainty on the water self-sufficiency ratio. Therefore, the main actions to reduce the uncertainty are adopting time series on the ambient temperature and relative humidity for the considered location.

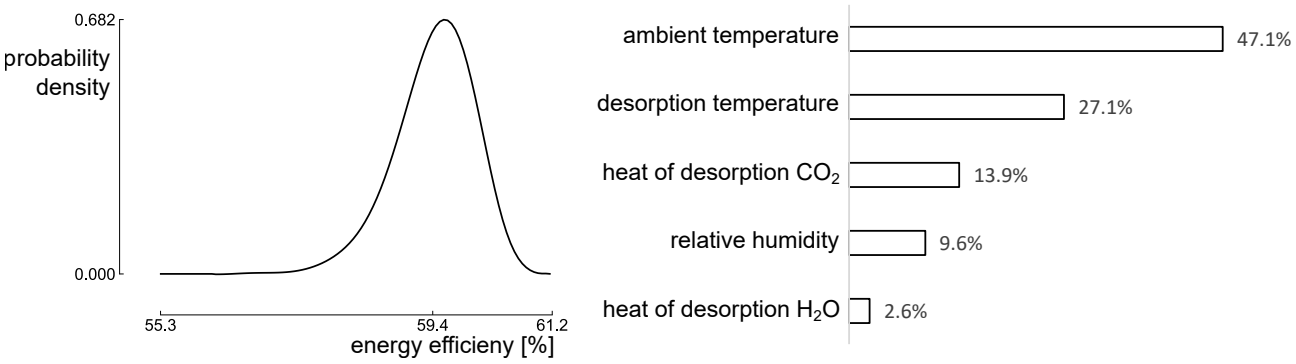

Figure 6: The distribution on the energy efficiency (mean = 59.4%, standard deviation = 0.61%) is mainly driven by the uncertainty on the ambient temperature, desorption temperature and the heat of desorption of CO_2.

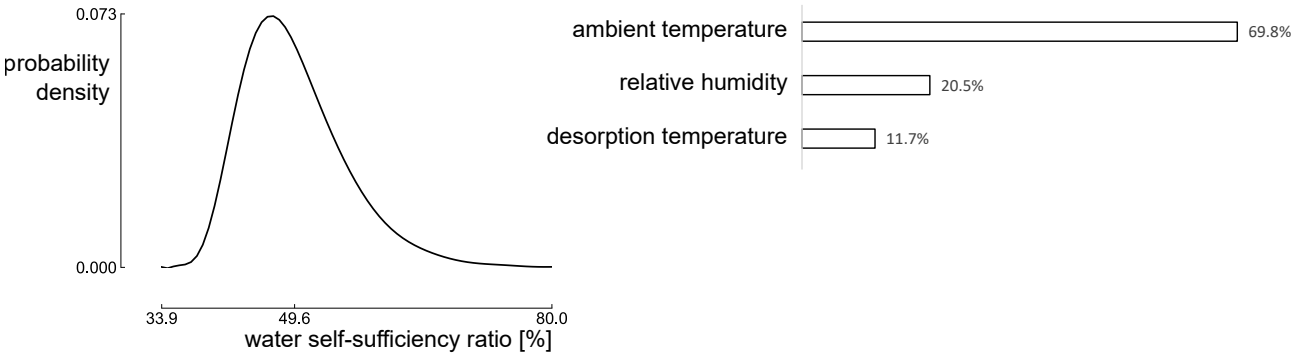

Figure 7: The uncertainty on the water self-sufficiency ratio (mean = 49.6%, standard deviation = 6.18%) is mainly defined by the uncertainty on the ambient conditions.

Similar to Figure 5, the desorption temperature is varied to evaluate the effect on the efficiency and water self-sufficiency ratio, considering the parametric uncertainties (Figure 8). The importance of the uncertainty on the ambient conditions reduces with an increasing nominal desorption temperature. Instead, the uncertainty on the heat of desorption and desorption temperature gains importance. The importance of the uncertainties on the water self-sufficiency ratio remains relatively stable concerning an increasing nominal desorption temperature. The standard deviation on the water self-sufficiency reaches its maximum value at 75 °C. This follows out of the fact that below a desorption temperature of 75 °C, an increasing amount of possible scenarios results in a water self-sufficiency ratio of 100 %, which reduces the standard deviation on the water self-sufficiency ratio.

4. Conclusion

Integrating Direct Air Capture (DAC) in a power-to-methane system unfolds several synergies, improving energy efficiency. Moreover, due to the co-adsorption of water in the DAC unit, the water self-sufficiency ratio of the system is improved. Under average ambient conditions for Belgium and a desorption temperature of 100 °C, an energy efficiency of 59.5 %, water self-sufficiency ratio of 48.8 % and an LCOE of 180 €/MWh are achieved. Reducing the desorption temperature improves the water self-sufficiency ratio, at the expense of a limited energy efficiency reduction. To illustrate, reducing the desorption temperature from 100 °C to 61 °C improves the water self-sufficiency ratio from 48.8 % to a water self-sufficient system. In contrast, the energy efficiency is reduced by 4 % absolute.

Several operating and ambient parameters are uncertain over the system lifetime. Considering these parametric uncertainties results in a limited uncertainty on the energy efficiency (mean = 59.4%, standard deviation = 0.61%), but a significant uncertainty on the water self-sufficiency ratio (mean = 49.6%, standard deviation = 6.18%). For the uncertainty on both quantities of interest, the uncertainty on the ambient conditions and desorption temperature are the main drivers. Therefore, adopting time series for the ambient conditions and stabilising the desorption temperature are the main actions to reduce the efficiency and water self-sufficiency ratio uncertainty.

The importance of the uncertainty on the ambient conditions reduces with an increasing nominal desorption temperature. Instead, the uncertainty on the heat of desorption and desorption temperature gains importance.

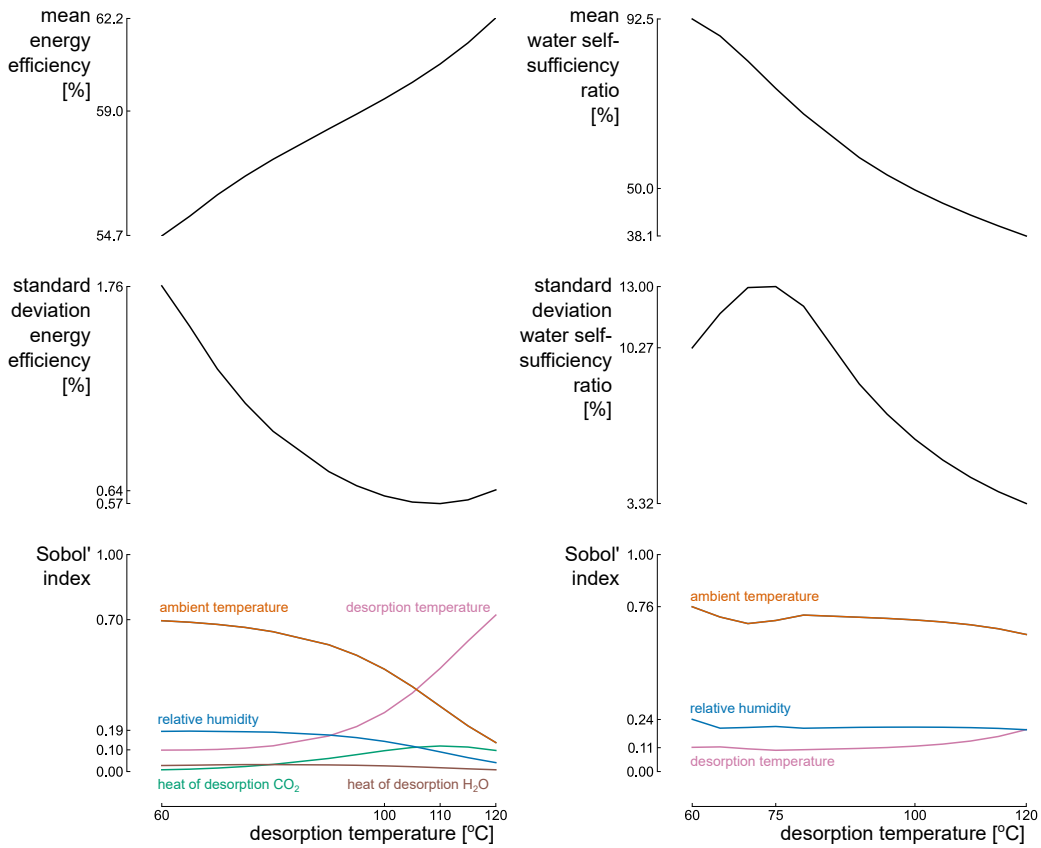

Figure 8: Increasing the ambient temperature improves the mean energy efficiency, but reduces the mean water self-sufficiency ratio. For the uncertainty on the energy efficiency, the importance of the uncertainty on the ambient conditions reduces with an increasing nominal desorption temperature. The standard deviation on the water self-sufficiency reaches its maximum value at 75 °C. This follows out of the fact that below a desorption temperature of 75 °C, an increasing amount of possible configurations results in a water self-sufficiency ratio of 100 %, which reduces the standard deviation on the water self-sufficiency ratio.

The importance of the uncertainties on the water self-sufficiency ratio remains relatively stable concerning an increasing nominal desorption temperature. The standard deviation on the water self-sufficiency reaches its maximum value at 75 %. This follows out of the fact that below a desorption temperature of 75 °C, an increasing amount of possible configurations results in a water self-sufficiency ratio of 100 %, which reduces the standard deviation on the water self-sufficiency ratio.

We will add an economic evaluation of the system in future works, with the dynamic operation of the components (PV, wind turbine, electrolyzer) and ambient conditions (ambient temperature, humidity).

Acknowledgments

The authors acknowledge the support from the Belgian federal Energy Transition Fund, project DRIVER.

References

[1] Lewandowska-Bernat A, Desideri U. Opportunities of power-to-gas technology in different energy systems architectures. Applied energy. 2018;228:57-67.

[2] Mertens J, Belmans R, Webber M. Why the Carbon-Neutral Energy Transition Will Imply the Use of Lots of Carbon. C. 2020;6(2):39.

[3] Rönsch S, Schneider J, Matthischke S, Schlüter M, Götz M, Lefebvre J, et al. Review on methanation–From fundamentals to current projects. Fuel. 2016;166:276-96.

[4] Buttler A, Spliethoff H. Current status of water electrolysis for energy storage, grid balancing and sector coupling via power-to-gas and power-to-liquids: A review. Renewable and Sustainable Energy Reviews. 2018;82:2440-54.

[5] Reiter G, Lindorfer J. Evaluating CO2 sources for power-to-gas applications–A case study for Austria. Journal of CO2 Utilization. 2015;10:40-9.

[6] Sabatino F, Grimm A, Gallucci F, van Sint Annaland M, Kramer GJ, Gazzani M. A comparative energy and costs assessment and optimization for direct air capture technologies. Joule. 2021;5(8):2047-76.

[7] Veneman R, Frigka N, Zhao W, Li Z, Kersten S, Brilman W. Adsorption of H2O and CO2 on supported amine sorbents. International journal of greenhouse gas control. 2015;41:268-75.

[8] Drechsler C, Agar DW. Intensified integrated direct air capture-power-to-gas process based on H2O and CO2 from ambient air. Applied Energy. 2020;273:115076.

[9] Chauvy R, Dubois L, Lybaert P, Thomas D, De Weireld G. Production of synthetic natural gas from industrial carbon dioxide. Applied Energy. 2020;260:114249.

[10] Kiani A, Jiang K, Feron P. Techno-economic assessment for CO2 capture from air using a conventional liquid-based absorption process. Frontiers in Energy Research. 2020;8:92.

[11] Sudret B. Polynomial chaos expansions and stochastic finite-element methods. Risk and Reliability in Geotechnical Engineering. 2014;Chap. 6(2003):265-300.

[12] Coppitters D, De Paepe W, Contino F. Robust design optimization of a photovoltaic-battery-heat pump system with thermal storage under aleatory and epistemic uncertainty. Energy. 2021:120692.

[13] Rixhon X, Limpens G, Coppitters D, Jeanmart H, Contino F. The Role of Electrofuels under Uncertainties for the Belgian Energy Transition. Energies. 2021;14(13):4027.

[14] Deng Z, Hu X, Lin X, Che Y, Xu L, Guo W. Data-driven state of charge estimation for lithium-ion battery packs based on Gaussian process regression. Energy. 2020;205:118000.

[15] Coppitters D, De Paepe W, Contino F. Robust design optimization and stochastic performance analysis of a grid-connected photovoltaic system with battery storage and hydrogen storage. Energy. 2020;213:118798.

[16] De Paepe W, Coppitters D, Abraham S, Tsirikoglou P, Ghorbaniasl G, Contino F. Robust Operational Optimization of a Typical micro Gas Turbine. Energy Procedia. 2019 feb;158:5795-803.

[17] Coppitters D, De Paepe W, Contino F. Surrogate-assisted robust design optimization and global sensitivity analysis of a directly coupled photovoltaic-electrolyzer system under techno-economic uncertainty. Applied Energy. 2019;248:310-20.

[18] Bell IH, Wronski J, Quoilin S, Lemort V. Pure and pseudo-pure fluid thermophysical property evaluation and the open-source thermophysical property library CoolProp. Industrial & engineering chemistry research. 2014;53(6):2498-508.

[19] Abdin Z, Webb CJ, Gray EM. Modelling and simulation of a proton exchange membrane (PEM) electrolyser cell. International Journal of Hydrogen Energy. 2015 oct;40(39):13243-57.

[20] Drechsler C, Agar DW. Investigation of water co-adsorption on the energy balance of solid sorbent based direct air capture processes. Energy. 2020;192:116587.

[21] Chauvy R, Verdonck D, Dubois L, Thomas D, De Weireld G. Techno-economic feasibility and sustainability of an integrated carbon capture and conversion process to synthetic natural gas. Journal of CO2 Utilization. 2021;47:101488.

[22] Coppitters D, Verleysen K, De Paepe W, Contino F. How can renewable hydrogen compete with diesel in public transport? Robust design optimization of a hydrogen refueling station under techno-economic and environmental uncertainty. Applied Energy. 2022;312:118694.

[23] Fasihi M, Efimova O, Breyer C. Techno-economic assessment of CO2 direct air capture plants. Journal of cleaner production. 2019;224:957-80.

[24] Berger M, Radu D, Detienne G, Deschuyteneer T, Richel A, Ernst D. Remote Renewable Hubs for Carbon-Neutral Synthetic Fuel Production. Frontiers in Energy Research. 2021:200.

[25] Staffell I, Pfenninger S. Using bias-corrected reanalysis to simulate current and future wind power output. Energy. 2016 nov;114:1224-39.

[26] Coppitters D, Tsirikoglou P, De Paepe W, Kyprianidis K, Kalfas A, Contino F. RHEIA: Robust design optimization of renewable Hydrogen and dErIved energy cArrier systems. Journal of Open Source Software. 2022;7(75):4370.